Author Manuscript

Author Manuscript

Author Manuscript

Author Manuscript

HHS Public Access

Author manuscript

J Chem Neuroanat. Author manuscript; available in PMC 2022 November 01.

Published in final edited form as:

J Chem Neuroanat. 2021 November ; 117: 102005. doi:10.1016/j.jchemneu.2021.102005.

Kv2.1 expression in giant reticular neurons of the postnatal mouse brain

Ting Ding[1,2,*], **Ana Maria Magarinos**[1,*], **Lee-Ming Kow**[1], **Teresa A. Milner**[3,4,^], **Donald W. Pfaff**[1,^]

[1]Laboratory of Neurobiology and Behavior, The Rockefeller University, 1230 York Avenue, New York, NY 10065

[2]Department of Medicine, Tongji Medical School, Huazhong University of Science and Technology, Wuhan, China 430064

[3]Feil Family Brain and Mind Research Institute, Weill Cornell Medicine, 407 East 61st Street, New York, NY 10065

[4]Harold and Milliken Hatch Laboratory of Neuroendocrinology, The Rockefeller University, 1230 York Avenue, New York, NY 10065

Abstract

Previous experiments charted the development of behavioral arousal in postnatal mice. From Postnatal Day 3 (P3) to Postnatal Day 6 (P6) mice (a) become significantly more active, “arousable”; and (b) in large reticular neurons, nucleus gigantocellularis (NGC), patch clamp recordings reveal a significantly increased ability to fire high frequency trains of action potentials as are associated with elevated cortical arousal. These action potential trains depend on delayed rectifiers such as Kv2.1. Here we report tracking the development of expression of a delayed rectifier, Kv2.1 in NGC neurons crucial for initiating CNS arousal. In tissue sections, light microscope immunohistochemistry revealed that expression of Kv2.1 in NGC neurons is greater at day P6 than at P3. Electron microscope immunohistochemistry revealed Kv2.1 labeling on

^**Corresponding authors.** Corresponding author: Teresa A. Milner, Ph.D., Feil Family Brain and Mind Research Institute, Weill Cornell Medicine, 407 East 61st Street, RM 307, New York, NY 10065 United States of America, Phone: (646) 962-8274, FAX: (646) 962-0535, tmilner@med.cornell.edu; Donald W. Pfaff: pfaff@rockefeller.edu, The Rockefeller University.

*These two leading authors made equivalent contributions to the research.

Author Contributions: DWP funding acquisition and designed research based on electrophysiological data of LMK; TAM. performed research and analyzed data; TD performed research and analyzed data which form the basis for this report; AMM began the research and taught methods to TD; TAM, LMK and DWP decided on the content of this report; DWP and TAM wrote the paper.

Publisher's Disclaimer: This is a PDF file of an unedited manuscript that has been accepted for publication. As a service to our customers we are providing this early version of the manuscript. The manuscript will undergo copyediting, typesetting, and review of the resulting proof before it is published in its final form. Please note that during the production process errors may be discovered which could affect the content, and all legal disclaimers that apply to the journal pertain.

Conflict of Interest: The authors declare no competing financial interests.

Ethics and Integrity Policies: The study contains no shared data. The authors have no conflict of interests to declare. The study adheres to Wiley’s publication ethics and integrity policies.

Ethics Statement

The submitted manuscript adheres to the Elsevier Ethics in Research and Publication guidelines.

All authors made a significant contribution to the study and have approved the final version of the manuscript.

The paper is based on original research that has not been published before.

Data and conclusions were generated by experiments and observations performed by the authors.

Author Manuscript Author Manuscript Author Manuscript Author Manuscript

the plasmalemmal surface of soma and dendrites, greater on P6 than P3. In brainstem reticular neuron cell culture, Kv2.1 immunocytochemistry increased monotonically from Days-In-Vitro 3 to 10, paralleling the ability of such neurons to fire action potential trains. The increase of Kv2.1 expression from P3 to P6, perhaps in conjunction with other delayed rectifier currents, could permit the ability to fire action potential trains in NGC neurons. Further work with genetically identified NGC neurons is indicated.

Keywords

behavioral arousal; reticular formation; nucleus gigantocellularis; Kv2.1; delayed rectifier; immunocytochemistry; immunohistochemistry

1. INTRODUCTION

Some of the unanswered questions about state changes in the central nervous system (CNS) focus on neuronal changes in very young animals as they begin to move and respond shortly after birth. Behavioral assays appropriate for neonatal animals are less numerous than those available for older animals, and a significant number of papers have focused on olfactory responses (Sullivan and Wilson, 1995; Alberts, 2007; Ménard et al., 2020). Arakawa (Arakawa, 2019) added comparisons across a larger range of sensorimotor adaptations, emotional states and a wider range of ages. For example, while newborn use olfactory or vomeronasal cues to guide their suckling behaviors, responses to auditory signals develop later (perhaps because ear canals do not open until after postnatal day (P) 10. The earliest somatosensory responses may be related to temperature control. Olfactory exposures starting on P1, to the odor of citral or control unscented bedding, paired with tactile reward, influenced sexual partner preferences in adulthood; neonatally citral-exposed males preferred citral scented females (Ménard et al., 2020). Even on the first postnatal day, infant rats show a preference for their home nest odor over clean shavings (Gregory and Pfaff, 1971).

The current histochemical project was motivated by our prior study intended to address a more elementary question: the simple capacity for initiating movement. In that study, mouse pups initiated movement on a flat smooth surface increasingly from P3 to P6, and this increase was correlated with the ability to fire trains of action potentials recorded in large medullary reticular neurons implicated in generalized CNS arousal (Liu et al., 2016). That is, the amount of time spent moving during a 15-minute test almost tripled from P3 to P6, and during subsequent patch-clamp recordings from nucleus gigantocellularis (NGC) neurons in hindbrain slices from the same age animals, the percent of cells which displayed the ability to fire action potential trains increased about five-fold. Because the ability to fire a high frequency of action potentials depended on delayed rectifier currents, e.g., Kv2.1, these currents are crucial for rapid repolarization of neurons to allow high frequency of firing (Swensen and Bean, 2003; Liu and Bean, 2014; Bishop et al., 2015). Thus, we (Liu et al., 2016) hypothesized that increased expression of at least one of these two delayed rectifier currents may explain our patch clamp recording results. In turn the

Author Manuscript Author Manuscript Author Manuscript Author Manuscript

patch clamp results could be causal to the behavioral results since NGC neurons send powerful descending reticulospinal signals.

This paper reports experiments designed to study the expression of delayed rectifier potassium channel Kv2.1 [for which a well-characterized antibody exists (Mandikian et al., 2014)] in these large medullary reticular neurons which are important for CNS arousal, and to test the hypothesis that expression increases from day P3 to P6 (Kow and Pfaff, 2021). In the medullary reticular formation, we focused on large neurons in NGC because their reticulospinal neuronal activities are correlated with CNS arousal (Martin et al., 2010; Gao et al., 2019; Pfaff, 2019) and some of them have bifurcating axons with long ascending and descending branches (Scheibel and Scheibel, 1961; Valverde, 1961b, a, 1962; Martin et al., 2011) as could support both the initiation of movement and cortical arousal. For quantification to test the hypothesis we used light microscope immunohistochemistry, whereas electron microscopic experiments were undertaken better to characterize the immunostaining. Results are consistent with but do not prove the notion of Kv2.1 participation in medullary reticular neuron-supported postnatal elevation of behavioral arousal, and do not rule out other ion channels as playing important roles.

2. MATERIALS AND METHODS

2.1 Experimental animals

C57BL/6/J mice (Jackson Laboratories, Bar Harbor ME) were maintained on a 12/12 light dark cycle with lights on at 7am and free access to water and food. Adult male and female animals were paired in the late afternoon to obtain timed pregnant dams and the morning when the formation of a vaginal plug was observed was counted as embryonic day 0. The day of animal birth was counted as P0. All experimental procedures were performed in accordance with the NIH guide for Care and Use of Laboratory Animals and approved by the Animal Care and Use Committee at The Rockefeller University.

2.2 Electrophysiological experiments

Patch clamp recordings to support the notion that Kv2.1 channels can influence delayed rectifier currents essential for action potential trains were carried out in cell cultures of dissociated neurons derived from dissections which centered on mouse NGC. Methods were similar to those used previously in our lab (Liu et al., 2016). Briefly, pregnant mice were anesthetized with isoflurane and embryonic (E) day 12.5 mice were removed from the uterus. The medial hindbrain tissue was dissected, neurons dissociated and then resuspended and cultured for up to 10 days (N = 29).

For whole-cell patch clamp recording and testing with Kv2 inhibitors, coverslips were superfused at ~1 ml/min with a HEPES-buffered artificial cerebrospinal fluid (HACSF), which consisted of (in mM): NaCl, 135; KCl, 5; $CaCl_2$, 1, $MgCl_2$, 1; HEPES, 10; Glucose, 10; pH 7.3. All recordings were performed at room temperature (RT). Electrode resistance was 5–7 MΩ when filled with an internal solution composed of (in mM): K-gluconate, 140; HEPES-K, 10; $MgCl_2$, 2; $NaHCO_3$, 0.6; Mg-ATP, 2; Na_2-ATP, 2; $CaCl_2$,1; Na-GTP, 0.3; EGTA, 5; and sucrose, 8.0. Whole-cell current or membrane potential (Vm) was amplified

Author Manuscript Author Manuscript Author Manuscript Author Manuscript

with Multiclamp 700B and recorded and analyzed with Clampex and Clampfit, respectively (Axon Instruments, San Jose, CA).

Once a neuron was successfully patched, the Vm was measured and a membrane test was carried out to measure access resistance (Ra), leak current and membrane capacitance (Cm). In order to obtain an accurate measure, a Cm averaging over 250 sweeps was used. When a patch met the criteria of Ra ≤ 20 mV and leak current ≤ 50 pA, the neuron was first subjected to current clamp steps (CCSt) to induce action potential. The holding current and pulse duration are, respectively, 0 pA and 1 sec, and the first level is −30 pA and is followed by 9 more sweeps at a 15-pA increment. The highest number of AP (AP#) was used as an index of the neuron's firing capability. The neuron was then tested for effects of Kv2 inhibitors, GTx or Resv, on K^+ currents, or on APTs. To study effects on K^+ currents, the bath perfusion was switched from HACSF to RTC (Regular HACSF plus Tetrodotoxin or TTX, a Na^+ channel blocker, at 0.5 μM, and Cadmium or Cd^{++}, a Ca^{++} channel blocker, at 200 μM). After 2.5 min, when AP was blocked, a single depolarizing pulse, which goes from the Vh of −70 mV to 80 mV for 1.5 sec, was administered every 30 sec until the evoked PPk (positive peak current) and SSt (steady state current) levels were stabilized. PPk is measured as the most depolarized point of the evoked trace and SSt is the average of the last 200 ms of the pulse. Leak current was also measured. When it increased beyond 50 pA on two consecutive tests, the experiment was terminated.

To test Guangxitoxin-1E (GTx) the bath perfusion was carefully stopped completely with the bath solution ending at a level that would make the bath volume approximately 1,500 microliters. The neuron was tested 6 times (for a total of 3 min) in the stationary bath and then 15 ml of 10 mM GTx was injected with a Gilson P20 pipettor. This would make the final concentration of GTx ~100 nM. This concentration was used by most, if not all, investigators (Liu and Bean, 2014; Fletcher et al., 2017) and appeared to be maximally effective. To avoid disturbing the patch, the tip of the pipette was in touch with the water-immersion lens just above the solution level and the GTx solution was injected in a way that allowed it to flow slowly down into the stationary bath. The neuron was then further tested for 6 times while the GTx solution was diffusing in the bath. In pilot experiments, it was found that the GTx effects stabilized within 3 min. Afterwards, the perfusion was resumed, and the test continued for up to 10 min to observe recovery from GTx effects.

For example, the hindbrain reticular neuron in Figure 2A was patch-clamped while being perfused at ~1 ml/min with regular artificial cerebrospinal fluid (R-ACSF). After the successful patch the neuron was tested repeatedly at a 30-sec interval with a depolarizing pulse (from a holding potential of −70 mV to 80 mV for 1.5 sec) to evoke whole-cell currents. Once the recorded currents were stable, the perfusion was switched to RTC (R-ACSF containing 0.5 mM Tetrodotoxin to block Na^+ channels, and 200 mM Cd^{++} to block Ca^{++} channels) and tested for 6 times. Then the perfusion was carefully and gradually reduced to stop to prevent subsequently added test agents from being washed away. The neuron was tested 5 times (light blue background). As the perfusion stopping had no effect on currents, the recording chamber was immediately injected with 15 ml of Veh (R-ACSF) and tested 6 more times (darker blue background) to verify that the act of injection and the Veh do not affect current levels. Next (red background), 15 ml of R-ACSF containing 10

Author Manuscript Author Manuscript Author Manuscript Author Manuscript

mM GTx was injected in the same way as Veh. Since the RTC in the recording chamber is approximately 1.5 ml, the final concentration of GTx is approximately 100 nM. In this and other similarly tested neurons, both SSt and PPk currents were reduced quickly by the GTx injection (red area). At the end (6^{th}) of the GTx tests, the perifusion was increased to the original rate and the wash out continued for 20 tests (10 min). there was recovery, albeit slow and incomplete.

Resveratrol (Resv) was tested with a slightly different procedure. After switching to RTC perfusion, the neuron was tested 6 times for pre-treatment control and then switched to RTC containing either Resv at 50 mM, a concentration near-maximal (Dong et al., 2013) or its vehicle, ethanol (ETOH, 0.025%). The neuron was tested 10 times (5 min) during the perfusion with test agents. In the case of ETOH administration, this was followed immediately by Resv perfusion and tested for another 5 min before switching back to RTC perfusion for 10 min to observe for recovery. When Resv was administered first, the perfusion was switched back to RTC for 10 min to allow for recovery before test with ETOH.

For example, both neurons B and C in Figure 2 were stimulated with the same protocol as for the neuron in Fig. 2A while perfused with RTC to block Na^+ and Ca^{++} channels. Resv (light red backgrounds) and ETOH (blue backgrounds) were applied by switching bath perfusion. **2A**, neither PPk nor SSt was affected by ETOH, but the perfusion with Resv reduced both currents. **2B**, Resv applied without prior ETOH application also reduced both PPk and SSt, indicating that Resv action does not require ETOH pretreatment. ETOH applied afterward had no effect. Both neurons showed slow and incomplete recovery.

2.3 Antibodies

anti-Kv2.1.—A mouse IgG_1 primary antibody to Kv2.1 (clone K89/34, #75-014) obtained from the University of California, Davis NIH NeuroMab Facility (RRID:AB_2877280) was used at a dilution of 1:500. This antibody was raised against a synthetic peptide, a 34 amino acid segment of the Kv2.1 protein (Mandikian et al., 2014) and was validated by comparison between results in wild-type and Kv2.1-KO mouse brain sections in which the KO obliterated immunostaining [(Mandikian et al., 2014) Figures 8-10)].

Anti-Tuj-1.—A mouse IgG_{2a} primary antibody to Tuj-1 (anti-beta III tubulin) was obtained from abcam, Eugene OR (catalogue #ab78078; RRID:AB_2256751). On Western blot of wildtype HAP1 cells, this antibody recognizes a band at 50 kDA; this band is absent in beta III Tubulin knock out samples (manufacturer's data sheet). Similarly, this antibody recognizes a 50kDA band in mouse and rat brain tissue lysates (manufacturer's data sheet).

2.4 Immunofluorescence in neonatal sections

Male P3 and P6 mice (N = 6 per age) were deeply anesthetized with isoflurane and their brains were removed from skull and fixed for either 3 days in 4% PFA at 4°C with mild agitation. The brains were then transferred to 0.1M phosphate buffered saline (PBS) containing 30% sucrose and stored at 4°C for 2 days until cut. The blocks were sectioned coronally (50μm thick) on a sliding microtome (American Optical, Rochester NY, model

Author Manuscript Author Manuscript Author Manuscript Author Manuscript

860). The sections then were transferred to multiwells containing storage solution (30% sucrose, 30% ethylene glycol in 0.1M PB) and stored at −20°C until they were used.

Selected sections containing the NGC area (Fig. 1) were washed in PBS, and then incubated with 0.3% Triton X-100 (Sigma, St. Louis MO, cat # X-100) in PBS for 1 hr at room temperature (RT). Next, sections were incubated with blocking buffer (5% normal goat serum (Jackson Immuno Research Lab, Inc., Bar Harbor ME, cat # 005-000-121), 0.3% Triton X-100 in PBS for 2 h, RT; and washed again in PBS. Sections then were placed in blocking buffer containing anti-Kv2.1 antibody (1:500 dilution) and incubated at 4°C overnight with gentle agitation on a rotator shaker (70rpm). Sections were washed (3x15 min) in 0.3% Triton X-100 in PBS and then incubated goat anti-mouse IgG1 secondary antibody conjugated to fluorochrome Alexa Fluor 488 (1:1000, #AP124JA4, Life Technologies, Millipore Sigma, Burlington, MA) in 0.3% Triton/PBS for 2 hours, RT. Sections were washed (3x 15 min) in PBS and cellular nuclei were counter stained with Hoechst (34580, Sigma Aldrich, St. Louis) in PBS for 10 min. Sections were mounted on 1% gelatin coated slides and coverslipped with Prolong Gold (cat # P36930, RRID:SCR_015961; Life Technologies Corporation Waltham MA). After the mounting medium was cured, slides were stored at 4°C protected from light until they were photographed.

2.5 Electron Microscopic Immunocytochemistry

Male P3 and P6 mice (N = 3 per age) were processed for immunoperoxidase localization of Kv2.1 using previously described methods (Milner et al., 2011). Briefly, mice were deeply anesthetized with isoflurane, decapitated and their heads immersion fixed in 5 ml of 3.75% acrolein (Polysciences, Washington, PA) and 2% PFA (Electron Microscopy Sciences (EMS), Hatfield, PA) in 0.1 M phosphate buffer (PB, pH = 7.4) for 2 days. The heads were transferred to PB, the brains removed from the skull and the brainstem containing the NGC was cut into a coronal block (5 mm thick). Sections (50 μM thick) through the NGC (Hof et al., 2000) (centered 2 mm posterior to lambda, 1 mm off midline, 4 mm deep) were cut using a Vibratome (Leica Microsystems, Buffalo Grove, IL) and collected into 24-well plates containing PB. Sections were kept in a cryoprotectant solution (30% sucrose and 30% ethylene glycol in PB) at −20°C. To ensure identical immunolabeling between groups, the sections were coded with hole punches and placed in a single container (Pierce et al., 1999). Sections were incubated in 0.5% sodium borohydride in PB for 30 min to neutralize reactive aldehydes then rinsed 8-10 times in PB until gaseous bubbles disappeared.

Tissue sections were rinsed in 0.1 M Tris-buffered saline (TS; pH, 7.6) and blocked in 0.5% BSA in TS for 30 min. After rinsing in TS, sections were incubated in mouse anti-Kv2.1 antibody (1:1000) in 0.025% TritonX 100, 0.1% BSA and TS for 24 hours at room temperature (25°C) followed by an additional 4 days at 4°C on a rotator shaker at 145 rpm. Sections then were rinsed in TS and incubated in a 1:400 dilution of biotinylated goat-anti-mouse IgG (Jackson Immunoresearch Laboratories) for 30 min. Next, sections were rinsed in TS and incubated in avidin-biotin complex (ABC; Vectastain Elite kit, Vector Laboratories, Burlingame, CA) at half the manufacturer’s recommended dilution for 30 min.

Author Manuscript Author Manuscript Author Manuscript Author Manuscript

After rinsing in TS, the sections were reacted in 3,3'-diaminobenzidine (DAB; Millipore Sigma) in 3% H_2O_2 in TS for 8 min.

Tissue sections were incubated in 2% osmium tetroxide for one hour followed by washes of PB and dehydration through increasing concentrations of ethanol and propylene oxide prior to embedding in EMbed 812 (Cat. #14120; EMS). Ultrathin sections (about 70-72 nm thick) through the NGC were cut on a Leica UCT ultramicrotome and collected on 400 mesh thin-bar copper grids (T400-Cu; EMS). The grids , then were counterstained with UranyLess™ (Cat. #22409; EMS) and lead citrate (Cat. #22410; EMS).

Tissue sections containing the NGC were examined on a Tecnai Biotwin transmission electron microscope (FEI, Hillsboro, OR). Profiles were identified based on standard morphology (Peters, 1991). All peroxidase labeled profiles were photographed from three blocks from each age. Twenty five grid squares (75,625 mm^2) were analyzed from each block. The mean and SEM of each number of labeled profiles was determined for each age.

2.6 Immunocytochemistry on primary cultures

2.6.1 Embryonic hindbrain dissection and primary cell cultures: Pregnant females at 12.5 days post conception (E12) were euthanized by cervical dislocation. Using forceps, the uterus was dissected by pulling the uterine horns out of the abdominal cavity and the birth canal was cut. The uterine horns containing the embryo sacs were carefully transferred into a clean plastic dish containing ice-cold DB. The average number of embryos per pregnant female was 6-8.

Under a dissecting stereomicroscope (model 10298, Zeiss, Maple Grove, MN), each embryo sac was separated from the intact uterine horns. The embryos were transferred to a plastic dish containing fresh ice-cold DB. The embryonic hindbrains were dissected according to established procedures (Fantin et al., 2013) centering on the medullary reticular formation which contains the NGC, and they were transferred to one of the wells of a 24-multiwell plate containing fresh DB. The DB was replaced with 500 microliters of the enzymatic cell dissociation reagent (StemPro® Accutase, Thermo Fisher Scientific, Waltham MA) and the hindbrains then were mechanically dissociated by gently pipetting up and down approximately 30 times. The enzymatic digestion was stopped by adding 3 ml of standard medium containing Dulbecco's Modified Eagle's Medium, DMEM supplemented with 10% fetal bovine serum and 1% penicillin/streptomycin (all from Gibco). The resulting cell suspension was filtered through a tube fitted with a cell strainer snap cap (35 mm nylon mesh, Falcon), transfer to a 15 ml Falcon tube and further diluted with standard media to a final volume of 10 ml. An aliquot of the suspension was mixed with an equal volume of trypan blue and the viable cell yield (cells/ml) was estimated using a Neubauer chamber. The cell suspension was centrifuged at 200g for 4 min at room temperature. After discarding the supernatant, the resulting cell pellet was immediately resuspended in standard media to reach a cell density per well of $2x10^5$. The 24-multiwell plate (Corning, Millipore Sigma) containing the cells were incubated in an incubator at 37°C and 5% CO_2.

Author Manuscript Author Manuscript Author Manuscript Author Manuscript

Neurobasal serum-free medium consisting of neurobasal medium. 2% B27 Supplement, 1% Glutamax, and 1% penicillin/streptomycin was exchanged every 3 days over the course of all experiments.

2.6.2 Immunocytochemistry procedure: At days 3, 5, 7 and 10 days in vitro (DIV), coverslips containing the embryonic hindbrain cell cultures were rinsed 3X in phosphate-buffered saline (PBS) for 5 min per rinse and then fixed in 4% paraformaldehyde (PFA; Millipore Sigma) for 5 minutes at room temperature. For each DIV, N = 8. After rinsing with PBS, the cells were permeabilized with 0.1% Triton X-100 (Millipore Sigma) in PBS for 15 min, blocked with 5% normal goat serum (Life Technologies Corporation) for 2 hours and incubated overnight at 4°C with anti-Kv2.1 (1:1500 dilution). Cells were rinsed in PBS and then incubated for 2 hours at RT with donkey anti-mouse IgG secondary antibody conjugated to Alexa Fluor 488 (1:1000 dilution; Life Technologies, Millipore Sigma). For double immunolabeling, cells processed as above for single labeling of anti-Kv2.1 and then washed with PBS 3X in PBS for 10 min per rinse and incubated overnight at 4°C in anti-Tuj-1 (1:1000). Cells were rinsed in PBS and then incubated for 2 hours at room temperature with donkey anti-mouse IgG secondary antibody conjugated to Alexa Fluor 647 (1:1000, Life Technologies Corporation, Waltham MA cat #21240). As Kv2.1 and Tuj-1 are located in different cellular compartments, the two labels were clearly distinguishable. Finally, cellular nuclei were counter stained with Hoechst in PBS for 10 min. The labelled cells were examined and imaged using a wide-field fluorescence Axioplan 2 imaging upright microscope (Zeiss).

Data analysis for cell cultures.: A multi-wavelength cell scoring application module for Metamorph software (Molecular Devices, San Jose, CA) was used. Alexa 488 to label neurons), and Alexa 647 to label Kv2.1, and finally Hoechst 34580 to label nuclei. Each wavelength (red , green and blue channels, respectively) was analyzed and cells were assigned scoring values for the presence or absence of each marker.

2.7 Figure preparation

For immunofluorescent micrographs, brightness, contrast and sharpness were adjusted in Microsoft Powerpoint 2010. For electron micrographs, images were first imported into Adobe Photoshop 9.0 (RRID:SCR_014199) where resolution was increased to 300 dpi and levels and sharpness (using unsharp mask) were adjusted. Electron micrographs then were imported into Microsoft Powerpoint 2010, where changes to brightness, contrast, and sharpness were made. Image adjustments were applied to the entire image.

2.8 Statistics

Significance was set at $p < 0.05$. Error bars are reported as standard error of the mean. For light microscopic studies, statistical analyses (SPSS, RRID:SCR_019096; Chicago III.) was performed via one-way analysis of variance (ANOVA) tests after which a Tukey post-hoc test was used. For the electron microscopic analysis, a Welch corrected Students t-test was performed.

Author Manuscript Author Manuscript Author Manuscript Author Manuscript

3. RESULTS

3.1 Electrophysiological experiments

To obtain evidence that Kv2 channels in hindbrain reticular neurons affect delayed rectifier currents which support high frequency trains of action potentials, we used whole-cell patch recording experiments in conjunction with each of two Kv2 channel blockers, Guangxitoxin-1E (Herrington, 2007) and resveratrol (Dong et al., 2013). In these experiments a single depolarizing pulse was used, and we measured the evoked positive peak potassium current (PPk) and steady state potassium current (SSt) levels. PPk was measured at the most depolarized point of the evoked trace, and SSt was the average of the last 200 ms of the pulse. Both guangitoxin ($p < 001$; Fig. 2A) and resveratrol ($p < 0.0001$; Fig. 2B,C) significantly reduced SSt and PPk, delayed rectifier currents associated with trains of action potentials. Thus, the reduction of PPK and SST by blockers of the Kv2 family of delayed rectifier currents shows the importance of these currents in the hindbrain reticular neurons whose immunocytochemical results constitute the main subject of this paper.

3.2 Light microscopic immunohistochemistry

Coronal sections through the medullary reticular formation from P3 and P6 mice were labeled for Kv2.1. In tissue from both ages, Kv2.1 immunoreactivity was densest in the cyto plasm, particularly near the cell membrane. Quantitative analysis demonstrated that Kv2.1 immunohistochemical staining was greater on P6 than on P3, as shown by green fluorescence in Figure 3A and B. In particular, NGC sections from P6 mice compared to P3 mice had a higher percent of Kv2.1-labeled neurons ($p < 0.01$; Fig. 3C), a higher percent of Kv2.1-labeled area above a fixed threshold of green fluorescence ($p < 0.001$; Fig. 3D), and a higher average intensity of green fluorescence for Kv2.1 across the NGC microscopic field ($p < 0.05$; Fig 3E).

3.3 Electron microscopic immunochemistry

On average, with semi-quantitative measures, P3 mice had significantly fewer [$t(3.99)=5.2$; $p = 0065$] Kv2.1-labeled profiles compared to P6 mice in the NGC (P3: 6.3 ± 1.2; P6: 15 ± 1.15; $N = 3$ blocks per age). In both ages, Kv2.1 labeling was on the plasmalemmal surface of soma (Fig. 4 A,B) and dendrites (Fig. 3 C–F). In some dendrites, Kv2.1-labeling was associated with endomembranes (Fig. 4 C,E). Occasionally, small extensions (possibly axons) emanated from the labeled dendritic profiles (Fig. 4 E, F). In a P6 mouse, Kv2.1-labeling was observed at the dendrite-axon juncture (Fig. 4 F).

3.4 NGC neuronal culture

Because increasing numbers of DIV of NGC neurons (from DIV3 to DIV 10) are associated with greater ability to fire trains of action potentials (Kow and Pfaff, 2021), we hypothesized that immunofluorescent staining for Kv2.1 would correspondingly increase from DIV3 to DIV10.

Photomicrographs of immunocytochemistry for Kv2.1 in cells cultured for increasing numbers of DIV show differences between DIV3 (when NGC neurons rarely show trains

Author Manuscript Author Manuscript Author Manuscript Author Manuscript

of action potentials) and DIV10 (when they more frequently do so). At DIV3, very small numbers of cells show bright green fluorescence indicating Kv2.1(Fig. 5A), whereas at DIV10 Kv2.1 labeled cells are more common (Fig. 5B, rectangles). Quantitative analysis (Fig. 5C) was done using two different thresholds (NP250 and NP300) for fluorescence strength (to demonstrate the robustness of the finding) and shows that the significant, monotonic rise in the numbers of Kv2.1 positive cells from DIV3 to DIV10 was robust in both the NP250 and NP300 thresholds (both curves, $p < 0.001$).

4. DISCUSSION

The main hypothesis of this paper has been to see if we could track the development of expression of a delayed rectifier, Kv2.1 in giant reticular neurons crucial for initiating CNS arousal (Wu et al., 2007; Martin et al., 2010; Gao et al., 2019; Pfaff, 2019). The comparison of P3 to P6 was chosen because previous work (Liu et al., 2016) showed that during that 3 day neonatal period, mice (a) become significantly more active, “arousable”; and (b) in these giant reticular neurons, NGC patch clamp recordings reveal a significantly increased ability to fire high frequency trains of action potentials as are associated with elevated cortical arousal (Wu et al., 2007; Gao et al., 2019), and which depend on delayed rectifier currents (Swensen and Bean, 2003; Liu and Bean, 2014).

The results show that under a specified set of conditions of tissue preparation, indeed, expression of Kv2.1 in NGC neurons is greater at day P6 than at P3. The importance of this finding is that the expression difference could theoreticallly permit the ability to fire action potential trains in NGC neurons which are, in turn, critical to the postnatal development of CNS arousal. Further work with genetically identified neurons will add specificity to such findings.

4.1 Technical considerations.

There are some technical considerations in this project: First, the P3/P6 difference may be sensitive to methods of tissue preparation. However, our finding that the light and electron microscopic results, which were obtained under different fixation condition, were in agreement lessens this concern. Second, we acknowledge that the Alexa 488 IgG used to identify Tuj1 could also bind to Kv2.1. However, this would not have altered the conclusion of the experiment since the two markers were clearly located in different regions of the cells. Third, in the cell culture experiments, because of the difficulty of microdissections at embryonic age 12.5 days, some cells could be included which are not NGC neurons.

4.2 Outlook.

Some of the findings from this work are notable for two reasons. First, they were stimulated by considerations of an abstract nature, generalized CNS arousal [e.g., (Pfaff, 2019)] whose elevation shortly after birth permits the first behavioral whole-body movements the animal makes outside the womb/With that consideration in mind, this work attempts to translate those abstract considerations into a concrete histochemical question, the expression of a well-chosen potassium channel by arousal-related neurons. Second, the electron microscopic experiments support and expand the relevant conclusions from the light microscopic work.

Author Manuscript Author Manuscript Author Manuscript Author Manuscript

The plasma membrane labeling for Kv2.1 is appropriate to the hypothesis that increasing postnatal age or increasing number of days in vitro, permitting great Kv2.1 expression, would allow stronger delayed rectifier expression and thus more occurrences of behaviorally relevant potential action potential trains.

Nevertheless, this paper by itself does not answer all the relevant questions on this subject. When future work with antibodies for other channels with delayed rectifier properties becomes validated, work with those will be indicated. As well, other arousal-related neurons outside the reticular formation, notably in locus coeruleus, may also answer new parts of the question about how to relate abstract questions of CNS arousal to specific cellular mechanisms. Finally, new experiments with genetically identified neurons will add specificity to findings in this area of work.

5. Conclusions

In conclusion, these results support the main hypothesis, that elevations in Kv2.1 expression in NGC neurons parallel previous electrophysiological results (Liu et al., 2016) and the elevation of behavioral arousal. Future work with other delayed rectifier channels may add to this story when reagents become available.

Acknowledgments:

We thank Ms. Natalina Contoreggi for assistance with electron microscopic experiments and the Neuroanatomy EM Core at Weill Cornell Medicine for histological assistance and use of the electron microscope.

Funding:

Supported by NIH grants DA08259 and HL 136520 (T.A.M.); HD05751 and New York Neuroscience Foundation (D.W.P.)

Data availability:

This manuscript contains no shared data.

Abbreviations:

CCSt	current clamp steps
Cm	membrane capacitance
CNS	central nervous system
DB	dissection buffer
DIV	days in vitro
ETOH	ethanol
GTx	Guangxitoxin-1E
HACSF	HEPES-buffered artificial cerebrospinal fluid

Author Manuscript Author Manuscript Author Manuscript Author Manuscript

HBSS	Hanks balanced salt solution
NGC	Nucleus gigantocellularis
P	post-natal day
PBS	phosphate buffered saline
PFA	paraformaldehyde
PPk	positive peak current
Ra	access resistance
R-ACSF	regular artificial cerebrospinal fluid
Resv	resveratrol
RT	room temperature
SSt	steady state current
Vm	membrane potential

REFERENCES

Alberts JR (2007) Huddling by rat pups: ontogeny of individual and group behavior. Dev Psychobiol 49:22–32. [PubMed: 17186514]

Arakawa H (2019) Sensorimotor developmental factors influencing the performance of laboratory rodents on learning and memory. Behav Brain Res 375:112140. [PubMed: 31401145]

Bishop HI, Guan D, Bocksteins E, Parajuli LK, Murray KD, Cobb MM, Misonou H, Zito K, Foehring RC, Trimmer JS (2015) Distinct Cell- and Layer-Specific Expression Patterns and Independent Regulation of Kv2 Channel Subtypes in Cortical Pyramidal Neurons. J Neurosci 35:14922–14942. [PubMed: 26538660]

Dong WH, Chen JC, He YL, Xu JJ, Mei YA (2013) Resveratrol inhibits K(v)2.2 currents through the estrogen receptor GPR30-mediated PKC pathway. Am J Physiol Cell Physiol 305:C547–557. [PubMed: 23804203]

Fantin A, Vieira JM, Plein A, Maden CH, Ruhrberg C (2013) The embryonic mouse hindbrain as a qualitative and quantitative model for studying the molecular and cellular mechanisms of angiogenesis. Nat Protoc 8:418–429. [PubMed: 23424750]

Fletcher EV, Simon CM, Pagiazitis JG, Chalif JI, Vukojicic A, Drobac E, Wang X, Mentis GZ (2017) Reduced sensory synaptic excitation impairs motor neuron function via Kv2.1 in spinal muscular atrophy. Nat Neurosci 20:905–916. [PubMed: 28504671]

Gao S, Proekt A, Renier N, Calderon DP, Pfaff DW (2019) Activating an anterior nucleus gigantocellularis subpopulation triggers emergence from pharmacologically-induced coma in rodents. Nat Commun 10:2897. [PubMed: 31263107]

Gregory EH, Pfaff DW (1971) Development of olfactory-guided behavior in infant rats. Physiol Behav 6:573–576. [PubMed: 5149448]

Herrington J (2007) Gating modifier peptides as probes of pancreatic beta-cell physiology. Toxicon 49:231–238. [PubMed: 17101164]

Hof P, Young W, Bloom F, Belinchenko P, Ceilo M (2000) Comparative cytoarchitectonic atlas of the C57BL/6 and 129/SV mouse brains, 1 Edition. Amsterdam: Elsevier.

Kow LM, Pfaff DW (2021) Potassium channels and the development of arousal-relevant action potential trains in primary hindbrain neurons. Brain Research.

Author Manuscript Author Manuscript Author Manuscript Author Manuscript

Liu PW, Bean BP (2014) Kv2 channel regulation of action potential repolarization and firing patterns in superior cervical ganglion neurons and hippocampal CA1 pyramidal neurons. J Neurosci 34:4991–5002. [PubMed: 24695716]

Liu X, Pfaff DW, Calderon DP, Tabansky I, Wang X, Wang Y, Kow LM (2016) Development of Electrophysiological Properties of Nucleus Gigantocellularis Neurons Correlated with Increased CNS Arousal. Dev Neurosci 38:295–310. [PubMed: 27788521]

Mandikian D, Bocksteins E, Parajuli LK, Bishop HI, Cerda O, Shigemoto R, Trimmer JS (2014) Cell type-specific spatial and functional coupling between mammalian brain Kv2.1 K+ channels and ryanodine receptors. J Comp Neurol 522:3555–3574. [PubMed: 24962901]

Martin EM, Pavlides C, Pfaff D (2010) Multimodal sensory responses of nucleus reticularis gigantocellularis and the responses' relation to cortical and motor activation. J Neurophysiol 103:2326–2338. [PubMed: 20181730]

Martin EM, Devidze N, Shelley DN, Westberg L, Fontaine C, Pfaff DW (2011) Molecular and neuroanatomical characterization of single neurons in the mouse medullary gigantocellular reticular nucleus. J Comp Neurol 519:2574–2593. [PubMed: 21456014]

Milner TA, Waters EM, Robinson DC, Pierce JP (2011) Degenerating processes identified by electron microscopic immunocytochemical methods. Neurodegeneration, Methods and Protocols:23–59.

Ménard S, Gelez H, Jacubovitch M, Coria-Avila GA, Pfaus JG (2020) Appetitive olfactory conditioning in the neonatal male rat facilitates subsequent sexual partner preference. Psychoneuroendocrinology 121:104858. [PubMed: 32919208]

Peters A, Palay SL, Webster H.d. (1991) The fine structure of the nervous system: neurons and their supporting cells, 3 Edition. New York: Oxford University Press.

Pfaff D (2019) How brain arousal mechanisms work. Cambridge: University of Cambridge Press.

Pierce JP, Kurucz OS, Milner TA (1999) Morphometry of a peptidergic transmitter system: Dynorphin B-like immunoreactivity in the rat hippocampal mossy fiber pathway before and after seizures. Hippocampus 9:255–276. [PubMed: 10401641]

Scheibel M, Scheibel A (1961) Structural substrates for integrative patterns in the brainstem reticular core. In: The Reticular Formation of the Brain (J H, ed), pp 31–68. Boston, MA: Little Brown.

Sullivan RM, Wilson DA (1995) Dissociation of behavioral and neural correlates of early associative learning. Dev Psychobiol 28:213–219. [PubMed: 7621984]

Swensen AM, Bean BP (2003) Ionic mechanisms of burst firing in dissociated Purkinje neurons. J Neurosci 23:9650–9663. [PubMed: 14573545]

Valverde F (1961a) Reticular formation of the pons and medulla oblongata. A Golgi study. J Comp Neurol 116:71–99. [PubMed: 13779838]

Valverde F (1961b) A new type of cell in the lateral reticular formation of the brain stem. J Comp Neurol 117:189–195. [PubMed: 13924446]

Valverde F (1962) Reticular formation of the albino rat's brain stem cytoarchitecture and corticofugal connections. J Comp Neurol 119:25–53. [PubMed: 13924447]

Wu H-Y, Hsu F-C, Gleichman AJ, Baconguis I, Coulter DA, Lynch DR (2007) Fyn-mediated phosphorylation of NR2B Tyr-1336 controls calpain-mediated NR2B cleavage in neurons and heterologous systems. Journal of Biological Chemistry 282:20075–20087.

Author Manuscript Author Manuscript Author Manuscript Author Manuscript

Highlights

- Action potentials increase in nucleus gigantocellularis (NGC) neurons from P3 to P6.
- Kv2.1 in NGC neurons important for action potentials and thus for CNS arousal.
- Kv2.1 expression in NGC neurons increases from P3 to P6.
- Kv2.1 is on the plasmalemmal surface of NGC neurons.
- Expression is correlated with action potential trains and thus with arousal.

Author Manuscript Author Manuscript Author Manuscript Author Manuscript

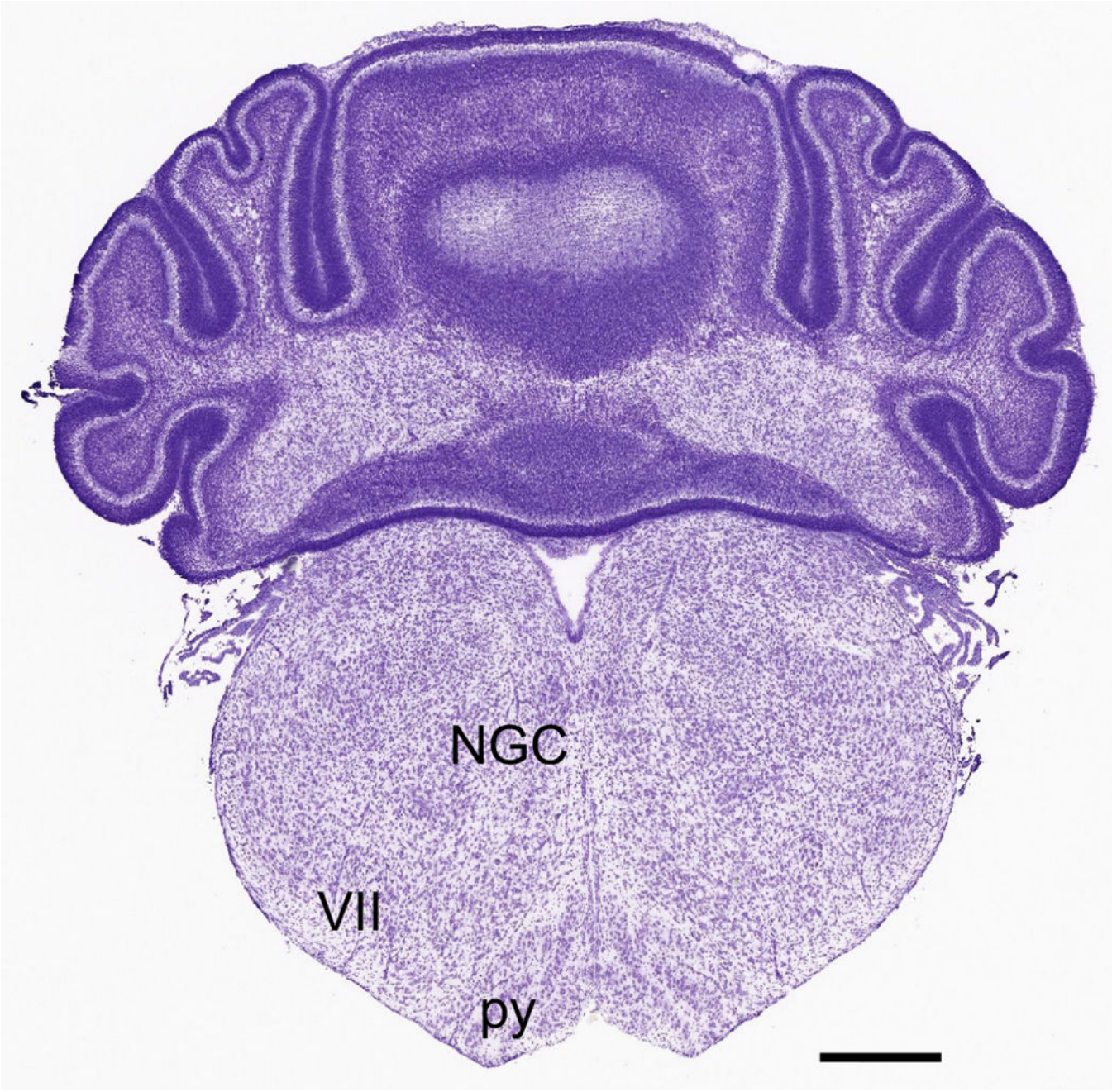

Fig. 1. Nucleus gigantocellularis (NGC) area in coronal section of P7 mouse brain.
NGC cells are found in the gigantocellular region of the brainstem. Py, pyramid; VII, 7th nerve. Bar = 500 mm. Image #139 Allen Developing Mouse Brain Atlas

Author Manuscript Author Manuscript Author Manuscript Author Manuscript

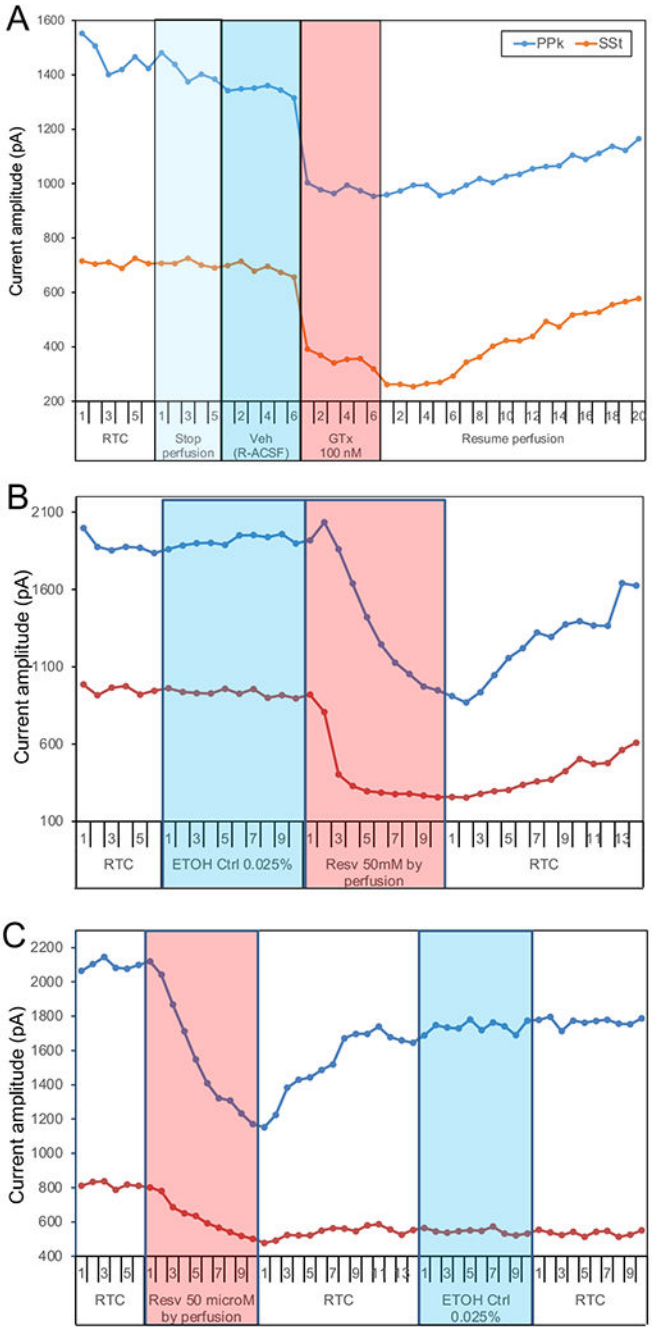

Fig. 2. Kv2 channels in NGC neurons affect delayed rectifier currents.

A. Guanxitoxin-1E (GTx; 100 nM; $p < 0.01$), but not its vehicle (Veh, R-ACSF), reduced both PPk (positive peak) and SSt (steady state) outward K^+ currents. **B,C**. Resveratrol (Resv; 50 mM $p < 0.0001$), but not its vehicle, ETOH (ethanol, 0.025%), also reduced PPk and SSt. A, n = 26 cells; B,C, n = 29 cells

Author Manuscript Author Manuscript Author Manuscript Author Manuscript

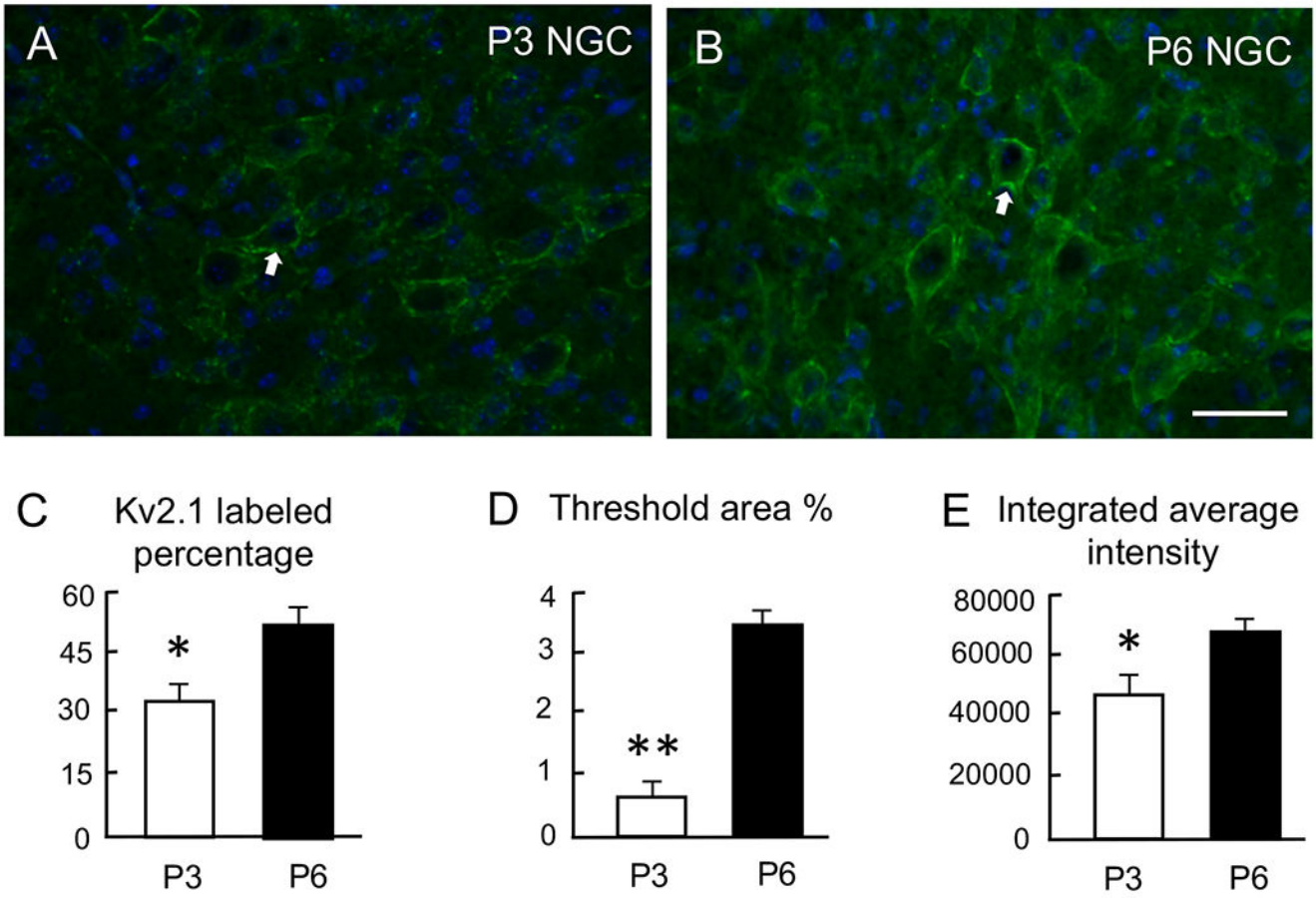

Fig. 3. Percent cells immmunostained for Kv2.1 in P6 compared to P3.

A,B. Example of Kv2.1 immunofluorescent labeling (green) in a coronal section of the NGC from P3 (A) and P6 (B) mice. Cellular nuclei were labeled with Hoechst stain (blue). Although P6 had more Kv2.1 labeling than P3 mice, in NGC from both ages Kv2.1 labeling was prominent in the cytoplasm, particularly near the cell membrane (**arrows)**. Bar = 40 mm **C.** The percent of cells immunofluorescently labeled for Kv2.1 were significantly higher ($p<0.01$) in P6 sections compared to P3 sections. **D.** The percent area labeled for Kv2.1 above a fixed threshold was significantly higher ($p<0.001$) in P6 than P3 NGC. **E.** The integrated average intensity of Kv2.1 immunofluorescence labeling was greater ($p<0.05$) in the NGC of P6 compared to P3 mice. N = 6 mice per age

Author Manuscript Author Manuscript Author Manuscript Author Manuscript

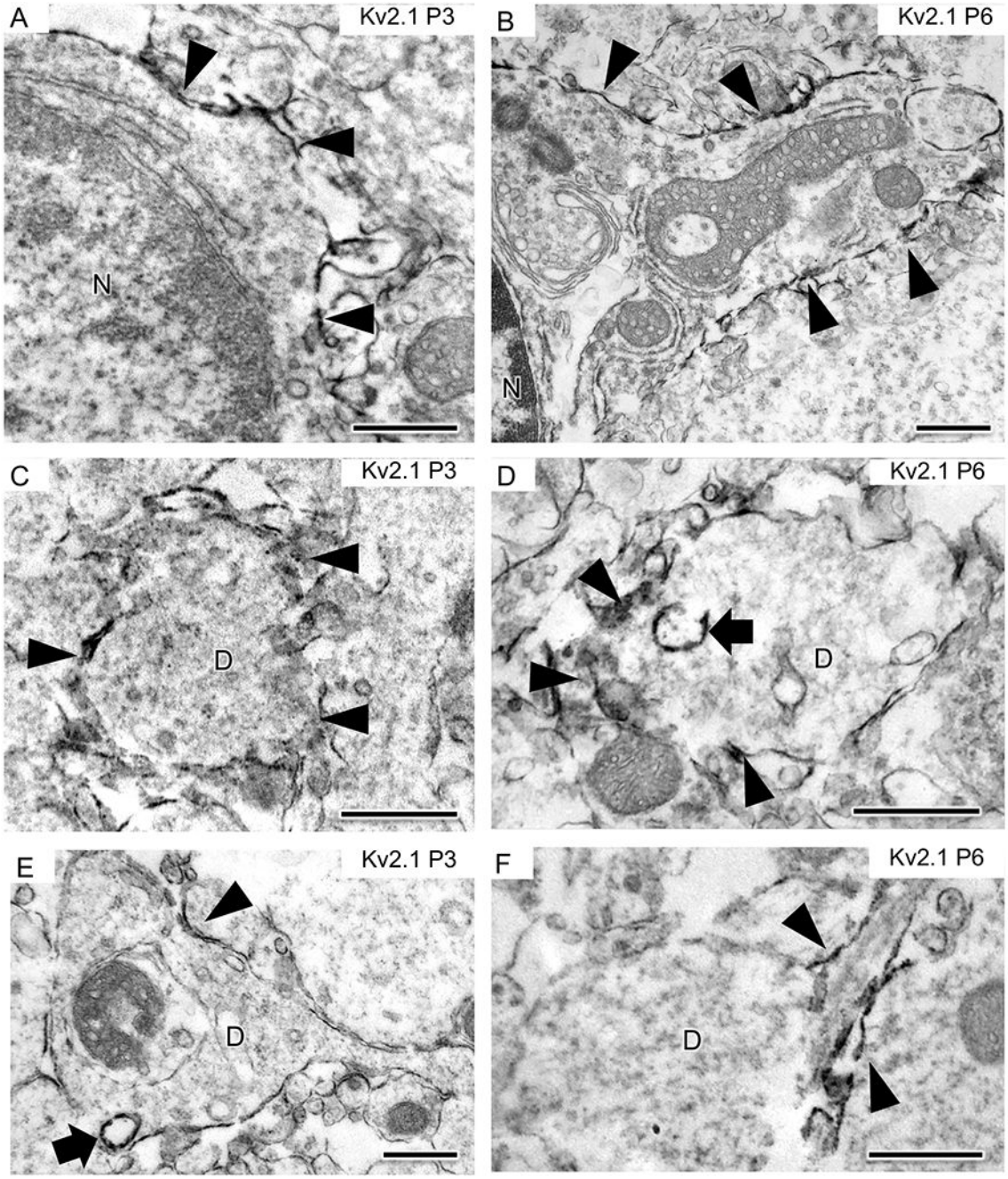

Fig. 4. Ultrastructural localization of Kv2.1 in the NGC of P3 and P6 mice.

A, B. Immunoperoxidase labeling for Kv2.1 (arrowheads0 is associated with the plasmalemma of neuronal somata in both P3 (A) and P6 (B) mice. C-F. Kv2.1 labeling is on the plasmalemma surface (arrowheads) of dendrites in both P3 (**C, E**) and P6 (**D, F**) mice. In both ages, Kv2.1 labeling is sometimes affiliated with endomembranes (arrows) within dendrites. Sometimes processes emanate from the labeled dendrites (**E, F**). D, dendrite; N, nucleus Bars = 500 nm.

Author Manuscript Author Manuscript Author Manuscript Author Manuscript

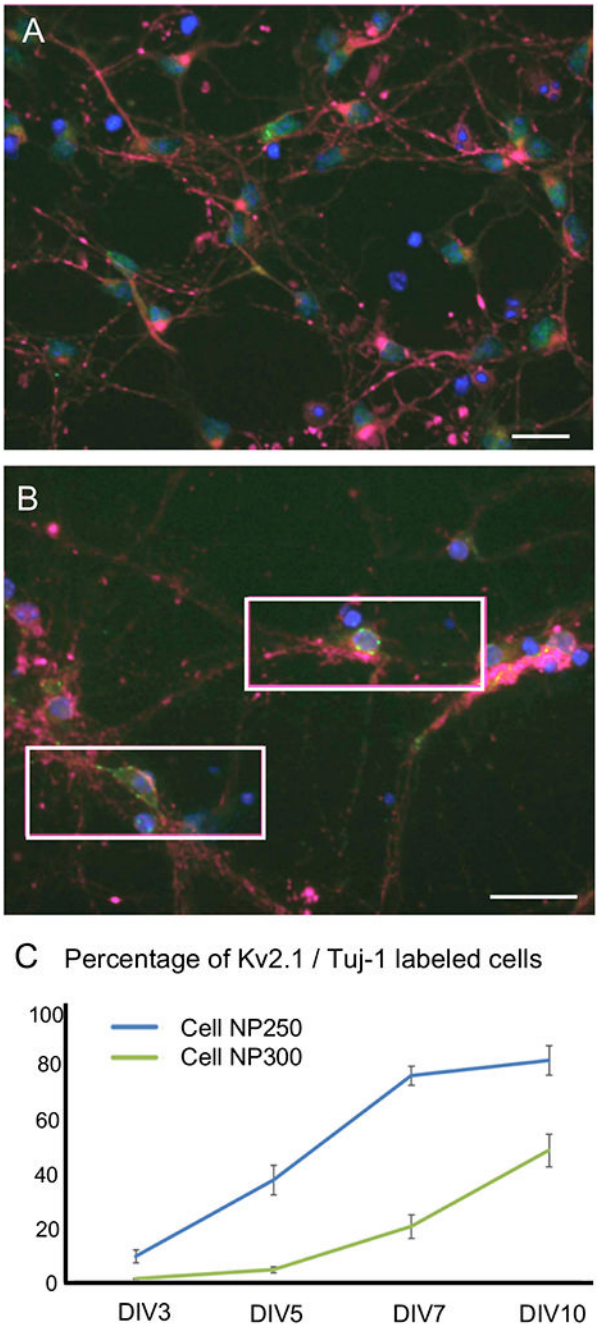

Fig. 5. Kv2.1 immunostaining increases as NGC cells progress from DIV3 to DIV10.

A,B. A. At DIV3, punctile labeling for Kv2.1 (green) was rarely detected among Tuj1-labeled cells (pseudo-colored magenta) and cell nuclei labeled with Hoechst stain (blue). **B.** Punctile Kv2.1 labeling in the cytoplasm was seen more frequently at DIV10 (in rectangles). Bars = 50 mm. **C.** Quantification of results from cell culture using two different thresholds (NP250 and NP300) for brightness of green fluorescence (to demonstrate that the result does not depend sensitively upon threshold chosen) showed a monotonic significant, monotonic

Author Manuscript Author Manuscript Author Manuscript Author Manuscript

rise in the numbers of Kv2.1 positive cells from DIV3 to DIV10 was robust (both curves, $p < 0.001$). N = 8 cell cultures per division